

CERN-TH/95-80

hep-ph/9504246

Future ν_τ Oscillation Experiments and Present Data

J. J. Gomez-Cadenas *

*Department of Physics and Astronomy, University of Massachusetts**Amherst, MA 01003, USA.*

M. C. Gonzalez-Garcia †

Theory Division, CERN, CH-1211 Geneva 23, Switzerland.

Abstract

Our goal in this paper is to examine the discovery potential of laboratory experiments searching for the oscillation $\nu_\mu(\nu_e) \rightarrow \nu_\tau$, in the light of recent data on solar and atmospheric neutrino experiments, which we analyse together with the most restrictive results from laboratory experiments on neutrino oscillations. In order to explain simultaneously *all* present results we use a four-neutrino framework, with an additional sterile neutrino. Our predictions are rather pessimistic for the upcoming experiments NOMAD and CHORUS, which, we find, are able to explore only a small area of the oscillation parameter space. On the other hand, the discovery potential of future experiments is much larger. We consider three examples. E803, which is approved to operate in the future Fermilab main injector beam line, MINOS, a proposed long-baseline experiment also using the Fermilab beam, and NAUSICAA, an improved detector which improves by an order of magnitude the performance of CHORUS/NOMAD and can be operated either at CERN or at Fermilab beams. We find that those experiments can cover a very substantial fraction of the oscillation parameter space, having thus a very good chance of discovering *both* $\nu_\mu \rightarrow \nu_\tau$ and $\nu_e \rightarrow \nu_\tau$ oscillation modes.

CERN-TH/95-80

*E-mail: jjgomez@phast.umass.edu or jjgomez@huhepl.harvard.edu. On leave from PPE Division, CERN, CH-1211 Geneva 23, Switzerland, and Departamento de Física Atómica y Nuclear, Universidad de Valencia, Spain

†E-mail: concha@vxcern.cern.ch (internet) or VXCERN::CONCHA (decnet).

April 1995

I. INTRODUCTION

Present data from solar and atmospheric neutrino experiments favour the hypothesis of neutrino oscillations. Nevertheless, this interpretation requires confirmation from further experiments, in particular from laboratory experiments. All solar neutrino experiments [1] find less ν_e than predicted theoretically. However, the uncertainties in the calculation of the solar neutrino flux may still be rather large [2] and new experiments [3,4] are being planned to further investigate the possible origin of the solar neutrino deficit. As for atmospheric neutrino experiments, two of them [5–7] measure a ratio ν_μ/ν_e smaller than expected from theoretical calculations. Here, in addition to the uncertainties on the estimation of the atmospheric neutrino flux and on the neutrino-nucleon cross section [8], one has to add the uncertainties due to the modest data sample. New experiments are also being planned in this area [4].

A complementary approach is to look for neutrino oscillations in laboratory experiments, where the experimental conditions, in particular the shape, energy, and flux of the neutrino beam are under control. A number of neutrino experiments have recently started taking data. These are the LSND experiment at Los Alamos [9], which looks for $\nu_\mu \rightarrow \nu_e$ oscillations, and the CHORUS [10] and NOMAD [11] experiments at CERN, which are primarily sensitive to $\nu_\mu(\nu_e) \rightarrow \nu_\tau$ oscillations. Recent data from LSND may be consistent with the existence of neutrino oscillations [12], although no formal claim has been made so far by the collaboration. First results from CHORUS and NOMAD should be available in 1996. In addition, a number of new $\nu_\mu(\nu_e) \rightarrow \nu_\tau$ oscillation experiments are being discussed. At Fermilab, a new, very intense $\nu_\mu(\nu_e)$ beam is planned to be available around the year 2001. Two complementary experiments are being discussed to benefit from this beam. These are E803 [13], a short-baseline experiment similar in design to CHORUS, and MINOS [14], a long-baseline experiment, which proposes to detect the neutrinos produced at Fermilab with a 10 Kton detector located in the Soudan mine, around 730 km away from the neutrino source. Furthermore, new experimental techniques are being studied to upgrade NOMAD

and CHORUS [15,16]. Ultimately, these new techniques could result in the design of new detectors able to improve the performance of NOMAD and CHORUS/E803 by one order of magnitude [17,18,15]. Such detector(s) could be operated either at CERN or at Fermilab beams.

In this paper we examine the prospects of success of all these experiments in the light of present data. CHORUS and NOMAD were conceived at a time when the dominant scenario for neutrino masses was consistent with very light ν_e , ν_μ and a ν_τ of about 10 eV constituting the hot component of the dark matter. This scenario arose as the most natural solution to explain the solar neutrino problem, simultaneously providing a candidate for the hot dark matter. However, present data no longer favour this simple scenario. Indeed, explaining the results from solar and atmospheric neutrino experiments in the usual three-neutrino framework is very difficult and requires a large degree of fine-tuning. One has to choose between throwing away part of the data and considering a larger scheme. The “minimal” scheme to explain *all* data without fine-tuning seems to be a four-neutrino framework ($\nu_e, \nu_\mu, \nu_\tau, \nu_s$) where ν_s is a sterile neutrino. Using this framework we perform a consistent analysis of the data from solar and atmospheric neutrino experiments as well as results on neutrino-oscillation laboratory experiments. This analysis enables us to re-assess the discovery potential of CHORUS and NOMAD as well as to study the prospects for the new experiments discussed above. We find that CHORUS and NOMAD have a rather marginal chance of discovering $\nu_\mu(\nu_e) \rightarrow \nu_\tau$ oscillations. However, the future ν_τ oscillation experiments have much better prospects since they cover a very large fraction of the oscillation parameter space.

The outline of the paper is as follows. In Sec. II we review the formalism for neutrino oscillation in a general multi-family framework. Section III is devoted to a summary of the present experimental status for solar and atmospheric neutrino experiments as well as accelerator and reactor neutrino oscillation experiments. The basic ingredients of the four-neutrino framework are presented in Sec. IV and the results of our analysis of the available experimental data, discussed in Sec. III, are displayed in Sec. V. Section VI describes

succinctly the upcoming and future ν_τ oscillation experiments while Sec. VII is dedicated to the study of the prospects for the discovery of ν_τ oscillations. Finally we present our conclusions in Sec. VIII.

II. FORMALISM

If neutrinos have a mass, the weak eigenstates ν_α produced in a weak interaction (i.e., an inverse beta reaction or a weak decay) will be, in general, a linear combination of the mass eigenstates ν_i

$$\nu_\alpha = \sum_{i=1}^n U_{\alpha i} \nu_i \quad (1)$$

where n is the number of neutrino species and U is a unitary mixing matrix.

After travelling a distance L , the neutrino can be detected in the charged-current (CC) interaction $\nu N' \rightarrow l_\beta N$ with a probability

$$P_{\alpha\beta} = \delta_{\alpha\beta} - 4 \sum_{i=1}^n \sum_{j=i+1}^n \text{Re}[U_{\alpha i} U_{\beta i}^* U_{\alpha j}^* U_{\beta j}] \sin^2 \left(\frac{\Delta_{ij}}{2} \right) \quad (2)$$

The probability, therefore, oscillates with oscillation lengths Δ_{ij} given by

$$\frac{\Delta_{ij}}{2} = 1.27 \frac{|m_i^2 - m_j^2|}{\text{eV}^2} \frac{L/E}{\text{m/MeV}} = 1.27 \frac{\Delta m_{ij}^2}{\text{eV}^2} \frac{L/E}{\text{m/MeV}} \quad (3)$$

where E is the neutrino energy. Each experimental set up has a different characteristic value of the ratio L/E and is thus most sensitive to oscillation lengths such that $\Delta m_{ij}^2 \approx 1/(L/E)$. The typical values of L/E are summarized in Table I.

In general neutrino beams are not monochromatic. Thus, rather than measuring $P_{\alpha\beta}$, the experiments are sensitive to the average probability

$$\begin{aligned} \langle P_{\alpha\beta} \rangle &= \frac{\int dE_\nu \frac{d\Phi}{dE_\nu} \sigma_{CC}(E_\nu) P_{\alpha\beta}(E_\nu) \epsilon(E_\nu)}{\int dE_\nu \frac{d\Phi}{dE_\nu} \sigma_{CC}(E_\nu) \epsilon(E_\nu)} \\ &= \delta_{\alpha,\beta} - 4 \sum_{i=1}^n \sum_{j=i+1}^n \text{Re}[U_{\alpha i} U_{\beta i}^* U_{\alpha j}^* U_{\beta j}] \langle \sin^2 \left(\frac{\Delta_{ij}}{2} \right) \rangle, \end{aligned} \quad (4)$$

where Φ is the neutrino energy spectrum, σ_{CC} is the cross section for the process in which the neutrino is detected (in general a CC interaction), and $\epsilon(E_\nu)$ is the detection efficiency for the experiment. For oscillation lengths such that $\Delta m_{ij}^2 \gg 1/(L/E)$ the oscillating phase will have been over many cycles before the detection and therefore it will have averaged to $\langle \sin^2(\Delta_{ij}/2) \rangle = 1/2$. On the other hand, for $\Delta m_{ij}^2 \ll 1/(L/E)$, the oscillation did not have time to give any effect and $\langle \sin^2(\Delta_{ij}/2) \rangle \approx 0$

For the case of two-neutrino oscillations the above expressions take the well known form

$$P_{\alpha\beta} = \delta_{\alpha\beta} - (2\delta_{\alpha\beta} - 1) \sin^2(2\theta) \langle \sin^2 \left(\frac{\Delta_{12}}{2} \right) \rangle \quad (5)$$

since

$$U = \begin{pmatrix} \cos \theta & \sin \theta \\ -\sin \theta & \cos \theta \end{pmatrix} \quad (6)$$

Most neutrino oscillation experiments present their result in the two-family mixing language as regions in the plane $(\Delta m^2, \sin^2(2\theta))$. Using the previous expression it is possible to translate their results into transition probabilities.

III. EXPERIMENTAL STATUS

A. Accelerator and Reactor Neutrino Experiments

There are two types of laboratory experiments to search for neutrino oscillations. In a disappearance experiment one looks for the attenuation of a neutrino beam primarily composed of a single flavour due to the mixing with other flavours. At present the most restrictive experiments of this kind are the reactor experiment at Bugey [19], which looks for ν_e disappearance, and the CDHSW experiment [20] at CERN, which searches for ν_μ disappearance. Both experiments show no indication of neutrino oscillation. Their results are presented as exclusion areas in the two-neutrino oscillation approximation in Fig. 1. We translate their results into limits on the transition probabilities:

$$\begin{aligned}
\langle P_{ee} \rangle &\gtrsim 0.93 \quad \text{from Bugey for } \Delta m^2 \gtrsim 4\text{eV}^2 \\
\langle P_{\mu\mu} \rangle &\gtrsim 0.95 \quad \text{from CDHSW}
\end{aligned}
\tag{7}$$

Both results are given at 90% CL. The maximum probability from Bugey is larger for smaller mass differences since the neutrino flux normalization can be better determined by the experiment. However, in the range of masses we are interested the relevant limit is the one given above.

In an appearance experiment one searches for interactions by neutrinos of a flavour not present in the neutrino beam. The most restrictive experiments are the E776 experiment at BNL [21] for the $\bar{\nu}_\mu \rightarrow \bar{\nu}_e$ channel and the E531 experiment at Fermilab [22] for the $\nu_\mu \rightarrow \nu_\tau$ channel. Neither of these experiments shows evidence for neutrino oscillation on those channels. Their results are also presented as exclusion areas in the two-neutrino oscillation approximation in Fig. 1. In terms of transition probabilities we find

$$\begin{aligned}
\langle P_{e\mu} \rangle &\lesssim 1.5 \times 10^{-3} \quad \text{from E776} \\
\langle P_{\mu\tau} \rangle &\lesssim 2 \times 10^{-3} \quad \text{from E531}
\end{aligned}
\tag{8}$$

at 90% CL.

Recently the Liquid Scintillator Neutrino Detector (LSND) experiment [12] has announced the observation of an anomaly that can be interpreted as neutrino oscillations in the channel $\bar{\nu}_\mu \rightarrow \bar{\nu}_e$. Most of the oscillation parameters required as explanation are already excluded by the E776 [21] and KARMEN [23] experiments. Their result can be marginally compatible with these previous results for $\Delta m^2 \approx 6\text{--}8 \text{ eV}^2$ and mixing $\sin^2(2\theta) \approx 3 \times 10^{-3}$. One must point out, however, that these ranges are still quite far from certain.

B. Solar Neutrinos

At the moment, evidence for a solar neutrino deficit comes from four experiments [1]. Putting all these results together seems to indicate that the solution to the problem is not astrophysical but must concern neutrino properties. The standard explanation for this deficit

would be the oscillation of ν_e to another neutrino species either active or sterile. Different analyses have been performed to find the allowed mass differences and mixing angles in the two-flavour approximation [24]. They all seem to agree that there are three possible solutions for the parameters:

- vacuum oscillations with $\Delta m_{ei}^2 = (0.5-1) \times 10^{-10}$ eV² and $\sin^2(2\theta) = 0.8-1$
- non-adiabatic-matter-enhanced oscillations via the MSW mechanism [25] with $\Delta m_{ei}^2 = (0.3-1.2) \times 10^{-5}$ eV² and $\sin^2(2\theta) = (0.4-1.2) \times 10^{-2}$, and
- large mixing via the MSW mechanism with $\Delta m_{ei}^2 = (0.3-3) \times 10^{-5}$ eV² and $\sin^2(2\theta) = 0.6-1$.

C. Atmospheric Neutrinos

Atmospheric neutrinos are produced when cosmic rays (primarily protons) hit the atmosphere and initiate atmospheric cascades. The mesons present in the cascade, decay leading to a flux of ν_e and ν_μ which reach the Earth and interact in the different neutrino detectors. Naively the expected ratio of ν_μ to ν_e is in the proportion 2 : 1, since the main reaction is $\pi \rightarrow \mu\nu_\mu$ followed by $\mu \rightarrow e\nu_\mu\nu_e$. However, the expected ratio of muon-like interactions to electron-like interactions in each experiment depends on the detector thresholds and efficiencies as well as on the expected neutrino fluxes.

Currently four experiments have observed atmospheric neutrino interactions. Two experiments use water-Cherenkov detectors, Kamiokande [5,6] and IMB [7], and have observed a ratio of ν_μ -induced events to ν_e -induced events smaller than the expected one. In particular Kamiokande has performed two different analyses for both sub-GeV neutrinos [5] and multi-GeV neutrinos [6], which show the same deficit. On the other hand, the results from the two iron calorimeter experiments, Fréjus [26] and NUSEX [27], appear to be in agreement with the predictions.

The results of the three most precise experiments are shown next. They are given as a double ratio $R_{\mu/e}/R_{\mu/e}^{MC}$ of experimental-to-expected ratio of muon-like to electron-like

events. The expected ratio $R_{\mu/e}^{MC}$ is obtained by Monte Carlo calculation of the atmospheric neutrino fluxes. We have used the expected fluxes from Gaisser *et al.* [28] (see also Ref. [29]) and Volkova [30] depending on the neutrino energies (see discussion in Sec. IV). Use of other flux calculations [31] would yield similar numbers.

$$\begin{aligned}
R_{\mu/e}/R_{\mu/e}^{MC} &= 0.55 \pm 0.11 && \text{for IMB} \\
R_{\mu/e}/R_{\mu/e}^{MC} &= 0.6 \pm 0.09 && \text{for Kamiokande sub-GeV} \\
R_{\mu/e}/R_{\mu/e}^{MC} &= 0.59 \pm 0.1 && \text{for Kamiokande multi-GeV} \\
R_{\mu/e}/R_{\mu/e}^{MC} &= 1.06 \pm 0.23 && \text{for Fréjus}
\end{aligned}
\tag{9}$$

The most plausible explanation for this anomaly is to suppose that ν_μ oscillates into another flavour. The oscillation $\nu_\mu \rightarrow \nu_e$ is almost completely ruled out by the reactor experiment data [19]. We are then left with $\nu_\mu \rightarrow \nu_\tau$ oscillations or oscillations to a sterile neutrino. The allowed range of masses and mixings in the two-family approximation from a global fit to the previous data is shown in Fig. 2.a and can be summarized as

$$\Delta m_{\mu i}^2 \gtrsim 2 \times 10^{-3} \quad \sin^2(2\theta) = 0.56-1 .
\tag{10}$$

The experiments have also observed an angular dependence on the value of these double ratios. The previous ranges were obtained without using the angular information. An analysis based on the angular dependence of the ratio leads to an upper limit on the possible value of Δm^2 , as can be seen from the Kamiokande multi-GeV analysis [6] and the IMB data [7]. However the allowed regions obtained from the best fit to these two sets of data are inconsistent at the 2σ level (see Fig. 5 in Refs. [6,45]). For this reason, we have chosen not to use the constraints arising from the angular dependence of the data in this analysis.

D. Dark Matter

There is increasing evidence that more than 90% of the mass in the Universe is dark and non-baryonic. Neutrinos, if massive, constitute a source for dark matter. Stable neutrinos can fill the Universe of hot dark matter if their masses add up to a maximum of about 30

eV. However, scenarios with only hot dark matter run into trouble in the explanation of the formation of structures on small scales of the Universe. On the other hand, models for structure formation favour the presence of cold dark matter. These models, however, fail in reproducing the data on the anisotropy of the microwave background. Currently, the best scenario to explain the data considers a mixture of 70% cold plus 30% hot dark matter [32]. This translates into an upper limit on neutrino masses [33]:

$$\sum_i m_{\nu_i} \lesssim 4\text{--}7 \text{ eV} . \quad (11)$$

IV. FOUR-FLAVOUR MODELS

Naive two-family counting shows that it is very difficult to fit all experimental information in Sec. III with three neutrino flavours [34,36], even without invoking the LSND data. The solar neutrino deficit could be due to $\nu_e \rightarrow \nu_\mu$ oscillations and the atmospheric neutrino deficit to $\nu_\mu \rightarrow \nu_\tau$ oscillations with the appropriate mass differences, for example with a mass hierarchy $m_{\nu_\tau} \gg m_{\nu_\mu}, m_{\nu_e}$. However, fitting this together with the present laboratory limits leaves no room for hot dark matter since the maximum allowed mass is of about $m_{\nu_\tau} < 0.7 \text{ eV}$ [29]. The only possible way out is to require that all three neutrinos are almost degenerate. This requires a certain degree of fine-tuning in order to explain the neutrinoless double beta decay data [36,37].¹

One could have $\nu_\mu \rightarrow \nu_\tau$ oscillations for the atmospheric neutrino deficit with almost degenerate ν_μ and ν_τ with masses $m_{\nu_\mu} = m_{\nu_\tau} \approx 2.5 \text{ eV}$ and $m_{\nu_e} \approx 0$ [36,39], but leaving out the explanation for the solar neutrino deficit. Or $m_{\nu_\mu} = m_{\nu_\tau} \approx 0 \text{ eV}$ and $m_{\nu_e} \approx 2.5$ to explain the atmospheric data but leaving unexplained both solar neutrino deficit and dark matter [39].

¹Notice that this scenario is also inconsistent with the oscillation parameters observed by LSND, should this experiment confirm their results

Also, it is possible to explain the solar neutrino deficit with $\nu_e \rightarrow \nu_{\tau(\mu)}$ with almost degenerate ν_e and $\nu_{\tau(\mu)}$ with masses $m_{\nu_e} = m_{\nu_{\tau(\mu)}} \approx 2.5$ eV and $m_{\nu_{\mu(\tau)}} \approx 0$, but leaving the atmospheric neutrino deficit unexplained [37,38]. Also $m_{\nu_e} = m_{\nu_{\tau(\mu)}} \approx 0$ eV and $m_{\nu_{\mu(\tau)}} \approx 2.5$ eV would explain the LSND data if confirmed but leaves both atmospheric and dark matter without explanation.

In the spirit of Pauli, one is tempted to introduce a new neutrino as a “desperate solution” [40] to understand all present data. The nature of such a particle is constrained by LEP results on the invisible Z width as well as data on the primordial ${}^4\text{He}$ abundance. Those rule out the existence of additional, light, active neutrinos. In consequence the fourth neutrino state must be sterile.

There are different mass patterns that one can construct with four such neutrinos to verify all the experimental constraints and evidence for neutrino oscillation and masses. We will assume a *natural* mass hierarchy with two light neutrinos with their main projection in the ν_s and ν_e directions and two heavy neutrinos with their largest component along the ν_μ and ν_τ flavours. We will also require that the sterile neutrino does not mix directly with the two heavy states. As we will see, this is necessary to verify the constraints from big bang nucleosynthesis [41]. Such a hierarchy appears naturally, for instance if one advocates an $L_e \pm L_\mu \mp L_\tau$ discrete symmetry for the mass matrix [34]. In Ref. [36] a similar mass pattern is also generated via a combination of see-saw mechanism and loop mechanism. Other possible patterns which explain all data such as some inverted mass schemes [37] require a somehow large degree of fine-tuning to explain the absence of neutrinoless double beta decay.

For any matrix presenting this *natural* mass hierarchy, the mixing matrix can be parametrized in a general way as ²

²A similar mass matrix is also introduced in Ref. [35].

$$U = \begin{array}{c|cccc} & \nu_s & \nu_e & \nu_\mu & \nu_\tau \\ \hline \nu_1 & c_{es} & s_{es}c_{e\mu}c_{e\tau} & s_{es}s_{e\mu} & s_{es}c_{e\mu}s_{e\tau} \\ \nu_2 & -s_{es} & c_{es}c_{e\mu}c_{e\tau} & c_{es}s_{e\mu} & c_{es}c_{e\mu}s_{e\tau} \\ \nu_3 & 0 & -c_{\mu\tau}s_{e\mu}c_{e\tau} - s_{\mu\tau}s_{e\tau} & c_{\mu\tau}c_{e\mu} & -c_{\mu\tau}s_{e\mu}s_{e\tau} + s_{\mu\tau}c_{e\tau} \\ \nu_4 & 0 & s_{\mu\tau}s_{e\mu}c_{e\tau} - c_{\mu\tau}s_{e\tau} & -s_{\mu\tau}c_{e\mu} & s_{\mu\tau}s_{e\mu}s_{e\tau} + c_{\mu\tau}c_{e\tau} \end{array} \quad (12)$$

with $c_i = \cos \theta_i$ and $s_i = \sin \theta_i$. For the sake of simplicity we have assumed no CP violation in the lepton sector. In this approximation $m_1, m_2 \ll m_3, m_4$ and $|m_3^2 - m_4^2| \ll m_3^2, m_4^2$. Also, ν_3 and ν_4 constitute 30% of dark matter in the Universe. This implies $m_3 \simeq m_4 = 2\text{--}3.5$ eV. Such a mass pattern has been argued to yield satisfactory results in Cold+Hot Dark Matter scenarios [33]. We can define

$$\begin{aligned} \Delta m_{solar}^2 &= |m_1^2 - m_2^2| \\ \Delta m_{AT}^2 &= |m_3^2 - m_4^2| \\ \Delta M_{DM}^2 &= |m_1^2 - m_3^2| \simeq |m_1^2 - m_4^2| \simeq |m_2^2 - m_3^2| \simeq |m_2^2 - m_4^2| \simeq (4 - 10) \text{ eV}^2. \end{aligned} \quad (13)$$

Transition probabilities between the different flavours will now have contributions from the three oscillation lengths due to the three different mass differences in the problem which we will denote $\sin^2(\Delta_{solar}/2)$, $\sin^2(\Delta_{AT}/2)$, and $\sin^2(\Delta_{DM}/2)$, respectively. We are now ready to reanalyse the experimental data presented in Sec. III in the four-flavour framework considering the oscillations with the three different oscillation lengths.

V. GLOBAL ANALYSIS

A. Laboratory Experiments

Laboratory experiments are insensitive to oscillations due to the solar mass difference Δm_{solar}^2 . Also, for most of them the oscillation due to the dark matter mass difference will be averaged to 1/2. As a consequence the negative results presented in Sec. III will impose severe constraints on the mixing angles.

For the Bugey reactor experiment the relevant transition probability is the ν_e survival probability. For any value of the atmospheric mass difference this probability will always verify

$$0.93 \lesssim P_{ee}^{Bugey} \leq 1 - 2c_{e\mu}^2 c_{e\tau}^2 (1 - c_{e\mu}^2 c_{e\tau}^2) \Rightarrow c_{e\mu}^2 c_{e\tau}^2 \geq 0.96 . \quad (14)$$

For CDHSW the relevant probability is the ν_μ survival probability

$$0.95 \lesssim P_{\mu\mu}^{CDHSW} \leq 1 - \frac{1}{2} \sin^2(2\theta_{e\mu}) \Rightarrow \sin^2(2\theta_{e\mu}) \lesssim 0.1 . \quad (15)$$

For E776 the situation is somehow more involved, since the value of the oscillating phase $\langle \sin^2(\Delta_{DM}/2) \rangle$ varies in the range $\Delta_{DM} = 4\text{--}10 \text{ eV}^2$ due to the wiggles of the resolution function of the experiment (see Fig. 1). Also, the experiment is sensitive to the atmospheric mass difference:

$$1.5 \times 10^{-3} \geq P_{e\mu}^{E776} = \sin^2(2\theta_{e\mu}) c_{e\tau}^2 \sin^2\left(\frac{\Delta_{DM}}{2}\right) + \left[\frac{1}{2} \sin(2\theta_{\mu\tau}) \sin(2\theta_{e\mu}) \sin(2\theta_{e\tau}) \cos(2\theta_{\mu\tau}) c_{e\mu} - \sin^2(2\theta_{\mu\tau}) (s_{e\mu}^2 c_{e\tau}^2 - s_{e\tau}^2) c_{e\mu}^2\right] \sin^2\left(\frac{\Delta_{AT}}{2}\right) . \quad (16)$$

For any value of the atmospheric mass difference and the $\mu\tau$ mixing angle, the previous limit is verified if

$$\sin^2(2\theta_{e\mu}) c_{e\tau}^2 \leq (2\text{--}5) \times 10^{-3} \quad (17)$$

The limit from E531 on the mixings $e\mu$ and $e\tau$ is always less restrictive than the previous ones for any value of Δm_{AT}^2 and ΔM_{DM}^2 .

Combining these constraints we obtain that $e\mu$ and $e\tau$ mixings are constrained to

$$\begin{aligned} \sin^2(2\theta_{e\mu}) &\leq (2\text{--}5) \times 10^{-3} \\ \sin^2(2\theta_{e\tau}) &\leq 0.16 \end{aligned} \quad (18)$$

where the range of $\sin^2(2\theta_{e\mu})$ depends on the specific value of ΔM_{DM}^2 .

If we now turn to the effect due to the oscillation with Δ_{AT} , we can rewrite the relevant probabilities for the different experiments expanding in the small angles $e\mu$ and $e\tau$:

$$\begin{aligned}
P_{\mu\mu}^{CDHSW} &\simeq 1 - \frac{1}{2} \sin^2(2\theta_{e\mu}) - \sin^2(2\theta_{\mu\tau}) \sin^2\left(\frac{\Delta_{AT}}{2}\right) \\
P_{\mu\tau}^{E531} &\simeq \sin^2(2\theta_{\mu\tau}) c_{e\tau}^2 \sin^2\left(\frac{\Delta_{AT}}{2}\right) \\
P_{e\mu}^{776} &\simeq \sin^2(2\theta_{e\mu}) c_{e\tau}^2 \sin^2\left(\frac{\Delta_{DM}}{2}\right) + \sin^2(2\theta_{\mu\tau}) s_{e\tau}^2 \sin^2\left(\frac{\Delta_{AT}}{2}\right).
\end{aligned} \tag{19}$$

With the constraints in Eq. (18), the Bugey experiment is not sensitive to oscillations with Δ_{AT} .

In Figs. 2 and 3 we show the exclusion contours in $(\Delta m_{AT}^2, \sin^2(2\theta_{\mu\tau}))$ which are due to the three experiments for different allowed values of the $e\mu$ and $e\tau$ mixings.

B. Solar neutrinos

Different authors have considered the propagation of neutrinos in the framework of more-than-two-neutrino oscillations [29,42–44]. Rather than reanalysing the solar neutrino data we will follow and adapt the results in Ref. [29]. Following the approach of Ref. [43] we will express the transition probabilities in the framework of four neutrinos in terms of the two-family ones.

For the solar neutrino deficit the relevant transition probability is the ν_e survival probability. For solar neutrino distance and energies, both oscillations with the Δm_{AT}^2 and ΔM_{DM}^2 will have averaged to 1/2 and the survival probability in vacuum takes the form

$$P_{ee}^{solar} \simeq 1 - 2c_{e\mu}^2 c_{e\tau}^2 (1 - c_{e\mu}^2 c_{e\tau}^2) - c_{e\mu}^2 c_{e\tau}^2 \sin^2(2\theta_{es}) \langle \sin^2\left(\frac{\Delta_{solar}}{2}\right) \rangle, \tag{20}$$

where we have expanded in the small mixings $e\mu$ and $e\tau$. Given the constraints on the product $c_{e\mu}^2 c_{e\tau}^2$ (Eq. (14)), the effect of the new mixings is very small and the vacuum oscillation solution remains basically unchanged.

For propagation in matter we follow the notation given in Ref. [43]. Following a similar procedure we can write the transition probability in the four-neutrino scenario in terms of the transition probability for two neutrinos as

$$P_{ee}^{4\nu} = 1 - c_{e\mu}^2 c_{e\tau}^2 + c_{e\mu}^2 c_{e\tau}^2 P_{ee}^{2\nu}, \tag{21}$$

where $P_{ee}^{2\nu}$ is computed in the two-family case from the evolution equation in matter substituting the electron density N_e by $N_e c_{e\mu}^2 c_{e\tau}^2$. According to the results of Ref. [29], and taking into account Eq. (14), the two MSW solutions are still valid in the presence of the new mixings. The effect of the mixings appears to go in the direction of favouring the small mixing solution [29]. The large mixing solution is also in conflict with the constraints from big bang nucleosynthesis. As can be seen from Fig. 1 and Fig. 2 in Ref. [41] for $\nu_e - \nu_s$ oscillations this solution would lead to an excess on the primordial ${}^4\text{He}$ abundance excluded by the present data.

C. Atmospheric Neutrinos

There are in the literature several analyses of the atmospheric neutrino data in terms of neutrino oscillations in two-family and three-family scenarios [45,46,29], the last ones being mostly in the one-mass-dominance approximation. This approximation is not valid in our scheme since the atmospheric neutrino fluxes can show the effect of oscillations due to two oscillation lengths Δ_{AT} and Δ_{DM} . We reanalyse the data in Eq. (9), taking into account the effect of these two oscillations. In doing so we will follow the notation of Ref. [46].

In each experiment the number of μ events, N_μ , and of e events, N_e , in the presence of oscillations will be

$$N_\mu = N_{\mu\mu}^0 \langle P_{\mu\mu} \rangle + N_{e\mu}^0 \langle P_{e\mu} \rangle, \quad N_e = N_{ee}^0 \langle P_{ee} \rangle + N_{\mu e}^0 \langle P_{\mu e} \rangle, \quad (22)$$

where

$$N_{\alpha\beta}^0 = \int \frac{d^2\Phi_\alpha}{dE_\nu d\cos\theta_\nu} \frac{d\sigma}{dE_\beta} \epsilon(E_\beta) dE_\nu dE_\beta d(\cos\theta_\nu) \quad (23)$$

and

$$\langle P_{\alpha\beta} \rangle = \frac{1}{N_{\alpha\beta}^0} \int \frac{d^2\Phi_\alpha}{dE_\nu d\cos\theta_\nu} P_{\alpha\beta} \frac{d\sigma}{dE_\beta} \epsilon(E_\beta) dE_\nu dE_\beta d(\cos\theta_\nu). \quad (24)$$

Here E_ν is the neutrino energy and Φ_α is the flux of atmospheric neutrinos ν_α ; E_β is the final charged lepton energy and $\epsilon(E_\beta)$ is the detection efficiency for such charged lepton; σ is the interaction cross section $\nu N \rightarrow N' l$. The expected rate with no oscillation would be

$$R_{\mu/e}^{MC} = \frac{N_{\mu\mu}^0}{N_{ee}^0}. \quad (25)$$

The value of this ratio is different for each experiment as it depends on the threshold for the detected lepton energy as well as on the detection efficiency for the different lepton flavours. The double ratio $R_{\mu/e}/R_{\mu/e}^{MC}$ of the expected ratio of muon-like to electron-like events with oscillation to the expected ratio without oscillations is given by

$$\frac{R_{\mu/e}}{R_{\mu/e}^{MC}} = \frac{\langle P_{\mu\mu} \rangle + \frac{N_{e\mu}^0}{N_{\mu\mu}^0} \langle P_{e\mu} \rangle}{\langle P_{ee} \rangle + \frac{N_{\mu e}^0}{N_{ee}^0} \langle P_{\mu e} \rangle}. \quad (26)$$

We perform a global fit to the data in Eq. (9) using the neutrino fluxes from Ref. [28] for $E_\nu < 3$ GeV. For $E_\nu > 10$ GeV we use the fluxes from Ref. [30], and for energies in between the two fluxes are smoothly connected. We perform the integrals starting at the different thresholds of each experiment and include the published detection efficiencies [5–7,26]. For the neutrino interaction cross section the dominant process is the quasielastic cross section [47]. For larger neutrino energies (for Fréjus and Kamiokande multi-GeV analyses) one-pion and multipion cross sections become relevant and are included [48].

The results of our χ^2 fit are shown in Figs. 2 and 3. In Fig. 2 the results are shown for zero mixings $e\mu$ and $e\tau$ as in a two-family scenario. Figure 3 shows the effect of the inclusion of the mixings. As seen in the figure the inclusion of the $e\tau$ mixing leads to a more constrained area for the oscillation parameters. When mixing $e\mu$ and $e\tau$ are non-zero and taking into account the constraints in Eq. (18), Eq. (26) takes the form

$$\frac{R_{\mu/e}}{R_{\mu/e}^{MC}} \simeq 1 + \frac{1}{2} \sin^2(2\theta_{e\tau}) - \sin^2(2\theta_{\mu\tau}) \langle \sin^2(\frac{\Delta_{AT}}{2}) \rangle, \quad (27)$$

where we have used the fact that for atmospheric neutrino experiments $\langle \sin^2(\Delta_{solar}/2) \rangle = 0$ and $\langle \sin^2(\Delta_{DM}/2) \rangle = 1/2$. For the purpose of illustration we have used the approximation $N_{e\mu}^0/N_{\mu\mu}^0 = N_{ee}^0/N_{\mu e}^0 \simeq 0.5$. The effect of the $e\tau$ mixing in Eq. (27) is to increase the value of the double ratio. Therefore a larger amount of $\mu\tau$ oscillation is needed to account for the deficit. Due to the small values allowed, a non-zero mixing $e\mu$ does not modify the analysis of the atmospheric neutrino data provided that $(\Delta M_{DM}^2, \sin^2(2\theta_{e\mu}))$ are allowed by the E776 data (see Fig. 1).

VI. ν_τ OSCILLATION EXPERIMENTS

A. CHORUS and NOMAD

The two upcoming $\nu_\mu(\nu_e) \rightarrow \nu_\tau$ experiments, CHORUS and NOMAD, are ν_τ appearance experiments, i.e., they search for the appearance of ν_τ 's in the CERN SPS beam consisting primarily of ν_μ 's, with about 1% ν_e 's, as shown in Fig. 4 (solid lines) [10,11]. The mean energy of the ν_μ beam is around 30 GeV and the detectors are located approximately 800 m away from the beam source. The ν_τ contamination of the SPS beam is virtually zero.

CHORUS and NOMAD have complementary techniques to identify a τ lepton. The NOMAD experiment [11] distinguishes a ν_τ CC interaction from ordinary ν_μ or ν_e interactions by exploiting the fact that the τ lepton produced in a ν_τ CC interaction, decays emitting one or more neutrinos which result in a measurable amount of missing transverse momentum, in the general direction of the charged lepton. NOMAD is in essence an electronic bubble chamber, with a continuous target alternating panels of a light material and drift chambers, followed by a transition radiation detector and an electromagnetic calorimeter. All the above detectors are located inside a 0.4 T magnetic field. Thus NOMAD measures essentially all the charged tracks and photons in the event, which enables a good reconstruction of the transverse missing momentum magnitude and direction. CHORUS [10] on the other hand, seeks to observe the finite path of the τ on its emulsion target. At SPS energies, the τ mean decay length is about 1 mm, giving two distinctive signatures in CHORUS emulsion. One-prong decays result in a short track with a kink, while three-prong decays appear as a short track splitting in three. Thus CHORUS rely on purely vertex techniques to identify the τ . However, in order to reduce the number of events to be scanned, loose kinematical cuts are also applied. To this extent, the emulsion target is followed by a spectrometer and a compensating calorimeter. In the surviving events, tracks reconstructed in the spectrometer are extrapolated to the emulsions in order to determine where to scan.

The initial goal of the SPS is to deliver 2.4×10^{19} protons on target over two years to both

experiments. The intense neutrino beam allows very light detectors (NOMAD has a fiducial mass of near 3 t, while the emulsion target of CHORUS is 800 kg). The main characteristics of NOMAD and CHORUS as well as their expected performance are summarized in Table II.

B. Future ν_τ Experiments at CERN

There are a number of future $\nu_\mu(\nu_e) \rightarrow \nu_\tau$ experiments beyond CHORUS and NOMAD being discussed at present. In the more immediate future there exists the possibility of an extended run at the CERN SPS beam, spanning several years after the initial period. Several suggestions have been made to upgrade CHORUS and NOMAD. The upgrade proposed for CHORUS would go in the direction of substituting the emulsion target with an active target made of scintillating capillaries read-out by CCDS [16]. NOMAD, on the other hand, could be upgraded by adding an instrumented target made of a sandwich of passive, low- Z material (carbon or beryllium) and silicon detectors [15]. Ultimately, one would like a precise measurement of the event vertex, which, when combined with the event kinematics, results in a much improved sensitivity. Specifically, the sensitivity of the upgraded NOMAD detector could be improved by one order of magnitude [15]. A different experimental approach, suggested in [17], proposes a 100 t liquid- CH_4 TPC in a high magnetic field (2 t). The idea is to use the quasi-free protons provided by the CH_4 to completely constrain the kinematics of the ν_τ -proton collisions. One can determine the momentum of the outgoing neutrino in the case of a τ decay involving one neutrino, and reconstruct invariant masses. The τ signal would appear as a mass peak over a very low background reduced by cuts á la CHORUS/NOMAD.

As a specific example of this improved detector we have considered a suggestion to upgrade the NOMAD detector (see [15] where detailed calculations are carried out). We will refer to this future detector with the generic name of Neutrino Apparatus with Improved Capabilities (NAUSICAA). Such a device would permit τ detection using *both* kinematical

and vertex techniques. Neutrino interactions would occur in a target made of a sandwich of silicon detector and a light- Z material. The event vertex would be precisely measured using the silicon information. The target would be followed by several planes of drift chambers and a calorimeter, with the full detector inside a magnetic field of around 1 T. The detector performance is summarized in Table IV. NAUSICAA can effectively suppress the CC and Neutral Currents (NC) $\nu_\mu(\nu_e)$ backgrounds, thanks to the combination of two independent signatures of the τ , i.e., its “long” lifetime and its decays with neutrino emission.

Finally, there are several proposals for long-baseline experiments using the CERN SPS beam (see for example [49] and references therein).

C. Future ν_τ Experiments at FNAL

At Fermilab, a neutrino beam will be available when the main injector becomes operational, around the year 2001. Compared with the CERN SPS beam, the main injector will deliver a beam 50 times more intense, but with an average energy around one third of that of the SPS neutrinos [13,14] (see Fig. 4).

There are currently two experiments proposed to operate in this beam. One is a short-baseline experiment, E803 [13], very similar in design and fiducial mass to CHORUS. Nevertheless, E803 is foreseen to have a sensitivity ten times better than CHORUS, thanks essentially to a much larger data sample (in addition to a more intense beam, the experiment expects a 4-year run). MINOS [14] is a long-baseline experiment, which proposes two detectors, separated by 732 km. This experiment can perform several tests to look for a possible oscillation $\nu_\mu \rightarrow \nu_\tau$ in the small mass difference range. Of those, the most sensitive is the comparison of the fraction of CC-like (defined for ν_μ) and NC-like events (a ν_τ event, appears, except for the decay $\tau \rightarrow \mu\nu_\mu\nu_\tau$ as a neutral current in the Minos detector). The main characteristics and expected performance of E803 and MINOS are summarized in Table III.

Finally we will consider the possibility of installing the NAUSICAA detector (see Table

IV) as an alternative or a successor to E803 in the Fermilab beam.

VII. DISCOVERY POTENTIAL

We now turn to the study of the prospects for the discovery of ν_τ oscillations in the upcoming CERN experiments CHORUS and NOMAD, in the future experiment E803 at Fermilab as well as a possible improved experiment, NAUSICAA, operated both at CERN and Fermilab beam. As an example of long-baseline experiment we also analyse the prospects for MINOS.

After implementing the limits derived in Sec. V and considering the sensitivity of the experiments, one sees that for all facilities the only observable $\nu_e \rightarrow \nu_\tau$ transition oscillates with an oscillation length Δ_{DM} such that

$$P_{e\tau} \simeq \sin^2(2\theta_{e\tau}) \sin^2\left(\frac{\Delta_{DM}}{2}\right) \quad (28)$$

Figure 5 shows the regions accessible to the experiments in the $(\sin^2(2\theta_{e\tau}), \Delta M_{DM}^2)$ plane. As can be seen, the almost complete accessible range of parameters for the CERN experiments CHORUS and NOMAD is already excluded by the Bugey data in the favoured range for the mass difference due to dark matter considerations. E803 at Fermilab and NAUSICAA at CERN could observe these oscillations in the whole favoured range of ΔM_{DM}^2 , provided that $\sin^2(2\theta_{e\tau}) \gtrsim 3 \times 10^{-2}$. Furthermore, NAUSICAA operated at the Fermilab beam can go as low as $\sin^2(2\theta_{e\tau}) \gtrsim 4 \times 10^{-3}$. MINOS, being a ν_μ disappearance experiment is not sensitive to this oscillation.

For transitions $\nu_\mu \rightarrow \nu_\tau$ a four-neutrino framework predicts (unlike the naive two-family framework) *two* oscillations, dominated by the characteristic lengths Δ_{DM} and Δ_{AT} . All experiments are in principle sensitive to both oscillations depending on the values of the mixing angles

$$\begin{aligned} P_{\mu\tau}^{DM} &\simeq \sin^2(2\theta_{e\mu}) \sin^2(\theta_{e\tau}) \sin^2\left(\frac{\Delta_{DM}}{2}\right) \\ P_{\mu\tau}^{AT} &\simeq \sin^2(2\theta_{\mu\tau}) \cos^2(\theta_{e\tau}) \sin^2\left(\frac{\Delta_{AT}}{2}\right) \end{aligned} \quad (29)$$

In Fig. 6 we show the regions accessible in the $(\sin^2(2\theta_{e\tau}), \Delta M_{DM}^2)$ plane to the different experiments for an optimum value of the $e\tau$ mixing $\sin^2(2\theta_{e\tau}) = 0.16$. As seen in the figure, the whole parameter space accessible to the CERN experiments CHORUS and NOMAD is already ruled out by the *E776* data. *E803* and NAUSICAA at CERN can marginally see this oscillation in the favoured range for ΔM_{DM}^2 for maximum $e\tau$ mixing. In particular if the LSND data are confirmed, this oscillation could be observable at both experiments for this optimum value of the $e\tau$ mixing. For smaller values of the $e\tau$ mixing these oscillations became very marginal or invisible. NAUSICAA at Fermilab can observe this oscillation for $\sin^2(2\theta_{e\mu}) \sin^2(\theta_{e\tau}) \gtrsim (0.3-1) \times 10^{-4}$. If the LSND results are confirmed, the same oscillation could then be detected in NAUSICAA at Fermilab, provided $\sin^2(\theta_{e\tau}) \gtrsim 10^{-2}$. As seen in the figure the accessible range for MINOS is already excluded by the *E776* data.

Figure 7 shows the region accessible to the experiments in the $(\sin^2(2\theta_{\mu\tau}), \Delta m_{AT}^2)$ parameter space for different values of the other mixings. As seen in the figure, the possibility of observing this oscillation depends on the values of the $e\tau$ and $e\mu$ mixings. For zero $e\tau$ mixing, the oscillation can be observed by all experiments in the region allowed by all laboratory and atmospheric neutrino experiments (see Fig. 7.a). It must be pointed out, however, that CERN experiments can observe this oscillation very marginally only. For larger values of the $e\tau$ mixing the situation is almost the same as long as the $e\mu$ mixing remains zero. If both mixings take their maximum allowed value the whole parameter space for the CERN experiments is ruled out by the atmospheric and *E776* experiments data (see Fig. 7.b).

E803 and NAUSICAA at CERN can observe oscillations with $\Delta m_{AT}^2 \gtrsim 5 \times 10^{-2} \text{eV}^2$ for any allowed value of the $e\tau$ and $e\mu$ mixings. NAUSICAA operated at the Fermilab beam could access oscillations with $\Delta m_{AT}^2 \gtrsim (2 \times 10^{-2}) \text{eV}^2$.³ MINOS can reach mass differences

³There is even the possibility [50] that NAUSICAA can be operated at two points, near the beam and at a few tenths of km allowing a limit $\Delta m_{AT}^2 \gtrsim (3 \times 10^{-3}) \text{eV}^2$ sufficient to close the atmospheric window

as low as $\Delta m_{AT}^2 \gtrsim (10^{-3}) \text{ eV}^2$, closing down the allowed window for the atmospheric neutrino experiments.

VIII. CONCLUSION

In this paper we have studied the discovery potential of laboratory experiments searching for the oscillation $\nu_\mu(\nu_e) \rightarrow \nu_\tau$, after considering existing data on solar and atmospheric neutrino experiments as well as the results from laboratory experiments on neutrino oscillations. To understand all these results in a common framework, we have introduced a fourth sterile neutrino and we have performed a comprehensive reanalysis of the data in this four-neutrino scenario. As an outcome of this analysis we can predict the number of expected events at future ν_τ oscillations experiments at CERN and Fermilab for the allowed oscillation parameters. We find that at these facilities $\nu_e \rightarrow \nu_\tau$ oscillations are dominated by mass differences of the order of $\Delta M_{DM}^2 \simeq 4\text{--}10 \text{ eV}^2$ while $\nu_\mu \rightarrow \nu_\tau$ oscillations could occur with both ΔM_{DM}^2 and $\Delta m_{AT}^2 \simeq 0.3\text{--}10^{-3} \text{ eV}^2$.

Our predictions are rather pessimistic for the upcoming experiments NOMAD and CHORUS, which, we find, are able to explore only a small area of the oscillation parameter space in both $\nu_e \rightarrow \nu_\tau$ and $\nu_\mu \rightarrow \nu_\tau$ channels. The prospects are much better for future ν_τ experiments. E803 and/or an improved detector (NAUSICAA) at CERN can explore $\nu_e \rightarrow \nu_\tau$ with $\sin^2(2\theta_{e\tau}) \gtrsim 10^{-2}$. As for $\nu_\mu \rightarrow \nu_\tau$, the oscillations with ΔM_{DM}^2 could be observed at E803/NAUSICAA-CERN in the range favoured by the LSND results, while oscillations with Δm_{AT}^2 are accessible for mixing values allowed by the atmospheric neutrino data if $\Delta m_{AT}^2 \gtrsim 5 \times 10^{-2} \text{ eV}^2$.

The proposed long-baseline experiment MINOS at Fermilab has the unique potential of completely exploring the region dominated by Δm_{AT}^2 thus, if present atmospheric neutrino data are correct MINOS *must* observe the oscillation $\nu_\mu \rightarrow \nu_\tau$. Finally, a future high-performance detector such as NAUSICAA at Fermilab could have the potential of exploring a very sizeable region of the parameter space for all the oscillation modes. The $\nu_e \rightarrow \nu_\tau$,

oscillations could be detected in the limit $\sin^2(2\theta_{e\tau}) \sim 10^{-3}$ and $\Delta M_{DM}^2 \sim 10 \text{ eV}^2$; $\nu_\mu \rightarrow \nu_\tau$ oscillations dominated by ΔM_{DM}^2 could be detected in the limit $\sin^2(2\theta_{e\mu}) \sim 3 \times 10^{-4}$ and $\Delta M_{DM}^2 \sim 10 \text{ eV}^2$, and $\nu_\mu \rightarrow \nu_\tau$ oscillations dominated by Δm_{AT}^2 could be detected in the limit $\Delta m_{AT}^2 \sim 2 \times 10^{-2} (\sim 3 \times 10^{-3})$ and maximal mixing. Indeed, NAUSICAA has the potential to observe *both* $\nu_\mu \rightarrow \nu_\tau$ and $\nu_e \rightarrow \nu_\tau$ oscillations.

ACKNOWLEDGMENTS

We want to thank P. Lipari for providing us with the atmospheric neutrino fluxes. We acknowledge discussions with R. Vazquez, P. Hernandez, R. Sundrum and S. R. Mishra. J. G. -C. acknowledges the hospitality of Harvard University.

REFERENCES

- [1] GALLEX Collaboration, Phys. Lett. **B327**, 377 (1994); SAGE Collaboration, Phys. Lett. **B328**, 234 (1994); Homestake Collaboration, Nucl. Phys. **B38** (Proc. Suppl.), 47 (1995); Kamiokande Collaboration, Nucl. Phys. **B38** (Proc. Suppl.), 55 (1995).
- [2] J. N. Bahcall and M. H. Pinsonneault, Rev. Mod. Phys. **64**, 885 (1992).
- [3] Borexino Collaboration, Gran Sasso National Laboratory Report LNSG-Report 94/99 Vol I (1994); Icarus Collaboration, Nucl. Phys. **B28A** (Proc. Suppl.), 486 (1992).
- [4] Y. Totsuka, SUPERKAMIOKANDE, ICCR-Report 227-90-20 (1990); G. T. Ewan, Sudbury Neutrino Observatory Proposal SNO-87-12 (1987).
- [5] Kamiokande Collaboration, H. S. Hirata *et al.*, Phys. Lett. **B205**, 416 (1988) and Phys. Lett. **B280**, 146 (1992).
- [6] Kamiokande Collaboration, Y. Fukuda *et al.*, Phys. Lett. **B335**, 237 (1994).
- [7] IMB Collaboration, D. Casper *et al.*, Phys. Rev. Lett. **66**, 2561 (1991); R. Becker-Szendy *et al.*, Phys. Rev. **D46**, 3720 (1992).
- [8] P. Lipari, M. Lusignoli, and F. Sartogo, Roma preprint 1072-1994 and hep-ph/9411341.
- [9] See for example W. C. Louis representing the LSND Collaboration, Nucl. Phys. **B38** (Proc. Suppl.), 229 (1995).
- [10] CHORUS Collaboration, N. Armenise *et al.*, CERN-SPSC/90-42 (1990).
- [11] NOMAD Collaboration, P. Astier *et al.*, CERN-SPSLC/91-21 (1991), CERN-SPSLC/91-48 (1991), SPSLC/P261 Add. 1 (1991).
- [12] H. Whyte, "Neutrino oscillations and neutrino mass", talk, MIT, 6 April 1995.
- [13] P-803 Proposal, Fermilab, October 1993.
- [14] P-875 Proposal, Fermilab, March, 1995.

- [15] J. J. Gomez-Cadenas, A. Bueno and J. A. Hernando, *A Proposal to Upgrade the NOMAD Detector* NOMAD/Memo 95-013(1995)
- [16] S. Buontempo *et al.*, CERN-PPE/94-142 (1994), submitted to Nucl. Instrum. Methods; G. Martellotti *et al.*, Nucl. Instrum. Methods **A315**, 177 (1992).
- [17] C. Rubbia, CERN-PPE/ 93-08 (1993), Proceedings of Conversaciones de Madrid, 5 Sept., 1992, El Escorial, Madrid.
- [18] K. Winter, CERN-EP/89-182, Proceedings of the Protvino UNK Workshop (1989), p.83.
- [19] B. Achkar *et al.*, Nucl. Phys. **B424**, 503 (1995).
- [20] CDHSW Collaboration, F. Didak *et al.*, Phys. Lett. **B134**, 281 (1984).
- [21] E776 Collaboration, L. Borodvsky *et al.*, Phys. Rev. Lett. **68**, 274 (1992).
- [22] E531 Collaboration, Phys. Rev. Lett. **57**, 2898 (1986).
- [23] B. Armbruster *et al.*, Nucl. Phys. **B38** (Proc. Suppl.), 235 (1995).
- [24] L. Krauss, E. Gates and M. White, Phys. Lett. **B299**, 94 (1993); P. I. Krastev and S. T. Petkov, Phys. Lett. **B299**, 99 (1993); N. Hata and P. Langacker, Phys. Rev. **D50**, 632 (1994).
- [25] S. P. Mikheyev and A. Yu. Smirnov, Yad. Fiz. **42**, 1441 (1985); L. Wolfenstein, Phys. Rev. **D17**, 2369 (1985).
- [26] Fréjus Collaboration, Ch. Berger *et al.*, Phys. Lett. **B227**, 489 (1989).
- [27] NUSEX Collaboration, M. Aglietta *et al.*, Europhys. Lett. **8**, 611 (1989).
- [28] T. K. Gaisser, T. Stanev and G. Barr, Phys. Rev. **D38**, 85 (1988) and Phys. Rev. **D39**, 3532 (1989).
- [29] G. L. Fogli, E. Lisi and D. Montanino, Phys. Rev. **D49**, 3626 (1994); CERN preprint

CERN-TH.7491/94.

- [30] L. V. Volkova, *Sov. J. Nucl. Phys.* **31**, 784 (1980) .
- [31] M. Honda, K. Hidaka, and S. Midorikawa, *Phys. Lett.* **B248**, 193 (1990); H. Lee and Y. S. Koh, *Nuovo Cim.* **105B**, 883 (1990).
- [32] E. L. Wright *et al.*, *Astrophys. J.* **396**, L13 (1992); M. Davis, F. J. Summers and D. Schlegel, *Nature* **359**, 393 (1992); A. N. Taylor and R. Rowan-Robinson, *ibid* **359**, 396 (1992); J. A. Holtzman, and J. R. Primack, *Astrophys. J.* **405**, 428 (1993).
- [33] J. R. Primack, J. Holtzman, A. Klypin, and D. O. Caldwell, UC Santa Cruz preprint SCIPP 94/28 and references therein.
- [34] J. Peltoniemi and J. W. F. Valle, *Nucl. Phys.* **B406**, 409 (1993)
- [35] J. Peltoniemi, D. Tommasini, and J. W. F. Valle, *Phys. Lett.* **B298**, 383 (1993); L. Bento and J. W. F. Valle, *Phys. Lett.* **B264**, 373 (1991).
- [36] D. O. Caldwell and R. N. Mohapatra, *Phys. Rev.* **D48**, 3259 (1993);
- [37] G. Raffelt and J. Silk, HEP-PH-9502306; G. M. Fuller, J. R. Primack and Y-Z. Qian, DOE-ER-40561-185.
- [38] D. O. Caldwell and R. N. Mohapatra, UC Santa Barbara preprint UCSB-HEP-95-1.
- [39] H. Minakata Tokyo Metropolitan University preprint TMUP-HEL-9502.
- [40] W. Pauli, on his famous letter presented to the Tübingen Meeting, in December, 1930 introduces the neutrino as a "desperate remedy".
- [41] X. Shi, D. N. Schramm and B. D. Fields, *Phys. Rev.* **D48**, 2563 (1993).
- [42] V. Barger, K. Whisnant, and R. J. N. Phillips, *Phys. Rev.* **D22**, 1636 (1980); *Phys. Rev.* **D43**, 1110 (1991).
- [43] T. K. Kuo and J. Pantaleone, *Phys. Rev.* **D35**, 3432 (1987).

- [44] A. De Rújula, M. Lusignoli, L. Maiani, S. T. Petkov and R. Petronzio, Nucl. Phys. **B168**, 54 (1980); H. Blumer and K. Kleinknecht, Phys. Lett. **B161**, 407 (1985).
- [45] E. W. Beier *et al.*, Phys. Lett. **B283**, 446 (1992); K. Hidaka, M. Honda and S. Midorikawa, Phys. Rev. Lett. **61**, 1537 (1988); Phys. Rev. **D44**, 3379 (1991).
- [46] V. Barger and K. Whisnant, Phys. Lett. **B209**, 365 (1988) .
- [47] C. L. Smith, Phys. Rep. **C3**, 261 (1972).
- [48] G. L. Fogli and G. Nardulli, Nucl. Phys. **B160**, 116 (1979); M. Nakahata *et al.*, J. Phys. Soc. Japan **55**, 3786 (1986).
- [49] J. P. Revol, CERN-PPE/93-84 (1993), Presented at the “Rencontres de Physique de la Vallé d’Aoste 1993”, 8 March, 1993.
- [50] S. Mishra, private communication.

TABLES

TABLE I. Characteristic values of L/E (m/MeV) for the different experiments considered in the analysis.

Experiment	$\langle L/E \rangle$ (m/MeV)
Solar neutrino	$\sim 10^{10}$
Atmospheric neutrino	$\sim 10^2$
Bugey	$\simeq 20$
CDHSW	$\simeq 0.8$
E776	$\simeq 0.4$
E531	$\simeq 0.04$
CHORUS/NOMAD	$\simeq 0.02$
E803	$\simeq 0.01$
MINOS	$\simeq 70$

TABLE II. Summary of the performance parameters for CHORUS and NOMAD.

	NOMAD	CHORUS
Target	Drift chamber panels	Emulsion
Mass (t)	~ 3	0.8
Target thickness (in X_0)	~ 1	~ 4
Initial run period (yr)	3	3
Number of CC Interactions	1.1×10^6	5×10^5
τ identification		
Technique	Pure kinematics	Pure vertex
Total efficiency in % ($EFF \times BR$)	~ 5	~ 10
Sensitivity:		
$P_{e\tau}$	1.3×10^{-2}	0.8×10^{-2}
$P_{\mu\tau}$	2×10^{-4}	1.4×10^{-4}

TABLE III. Summary of the performance parameters for E803 and MINOS.

	E803	MINOS
Mass (t)	~ 0.75	10,000
Target thickness (in X_0)	~ 3	Very Large
Initial run period (yr)	4	2
Number of CC interactions	$\sim 9 \times 10^6$	$\sim 10^5$
τ identification		
Technique	Pure vertex	Disappearance experiment (ratio NC/CC)
Total efficiency in % ($EFF \times BR$)	~ 10	~ 70
Sensitivity:		
$P_{e\tau}$	7×10^{-4}	–
$P_{\mu\tau}$	1.4×10^{-5}	0.012

TABLE IV. Summary of the performance parameters for NAUSICAA

	NAUSICAA (CERN)	NAUSICAA (FNAL)
Target	Silicon/Graphite	Silicon/Beryllium
Mass (t)	~ 1	~ 2
Target thickness (in X_0)	~ 1	~ 1
Initial run period (yr)	4	4
Number of CC interactions	1.3×10^6	2.4×10^7
τ identification		
Technique	Vertex and kinematics	Vertex and kinematics
Total efficiency in % ($EFF \times BR$)	~ 20	~ 10
Sensitivity:		
$P_{e\tau}$	7×10^{-4}	7×10^{-5}
$P_{\mu\tau}$	2×10^{-5}	2×10^{-6}

FIGURES

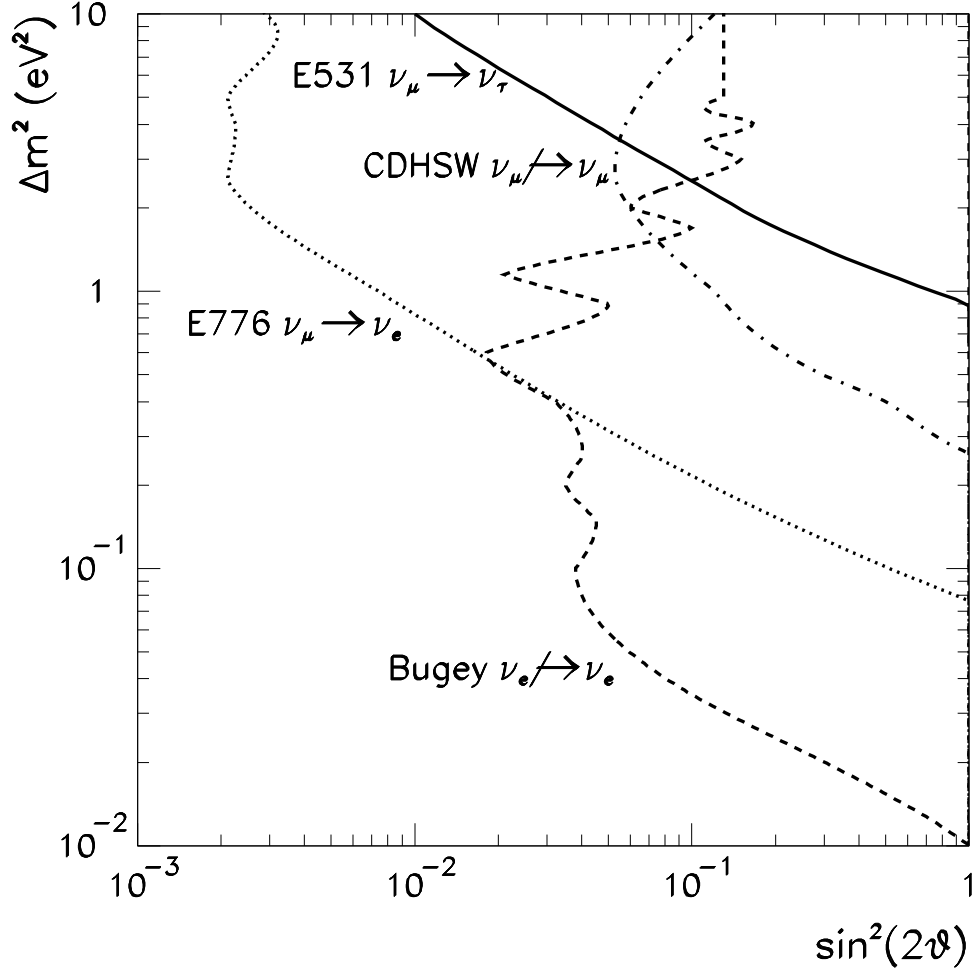
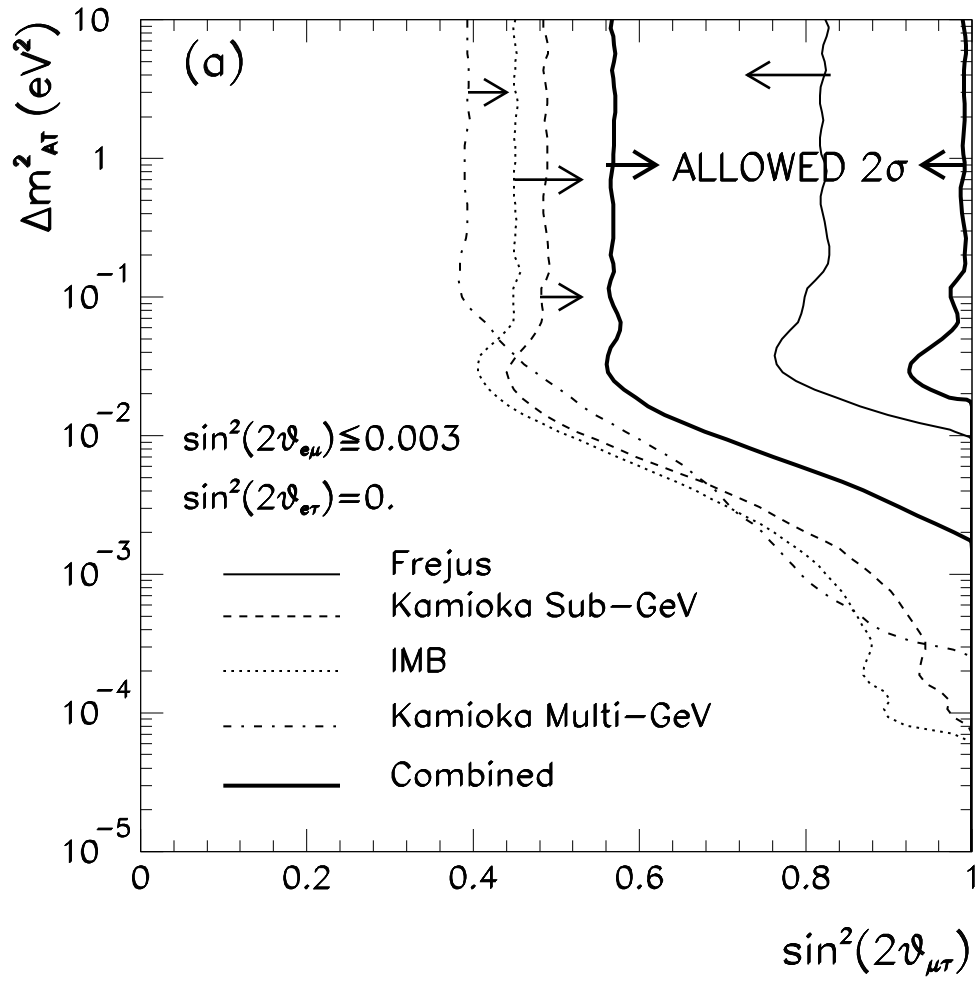


FIG. 1. 90% CL exclusion contours for different reactor and accelerator experiments in the two-family mixing approximation: E531 $\nu_\mu \rightarrow \nu_\tau$ appearance experiment (solid line), Bugey $\nu_e \not\rightarrow \nu_e$ disappearance experiment (dashed line), E776 $\nu_\mu \rightarrow \nu_e$ appearance experiment (dotted line), and CDHSW $\nu_\mu \not\rightarrow \nu_\mu$ disappearance experiment (dot-dashed line). The allowed regions lie below the curves.



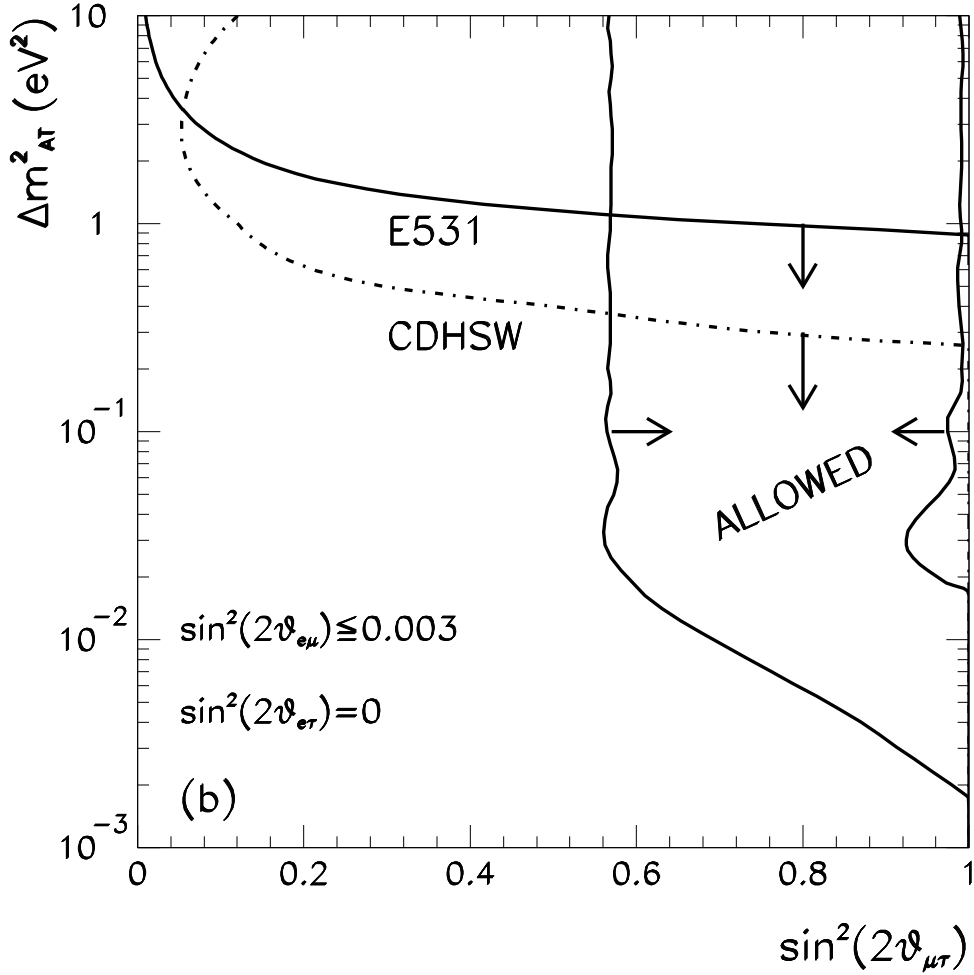
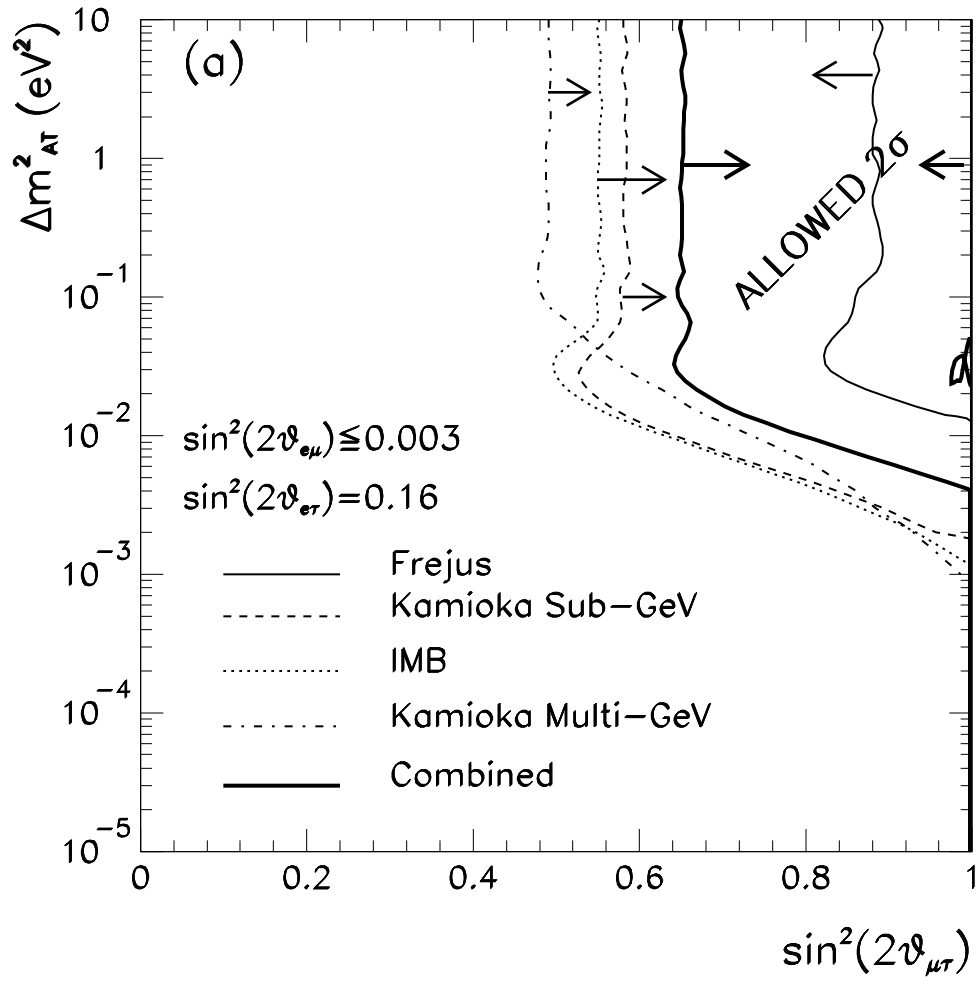
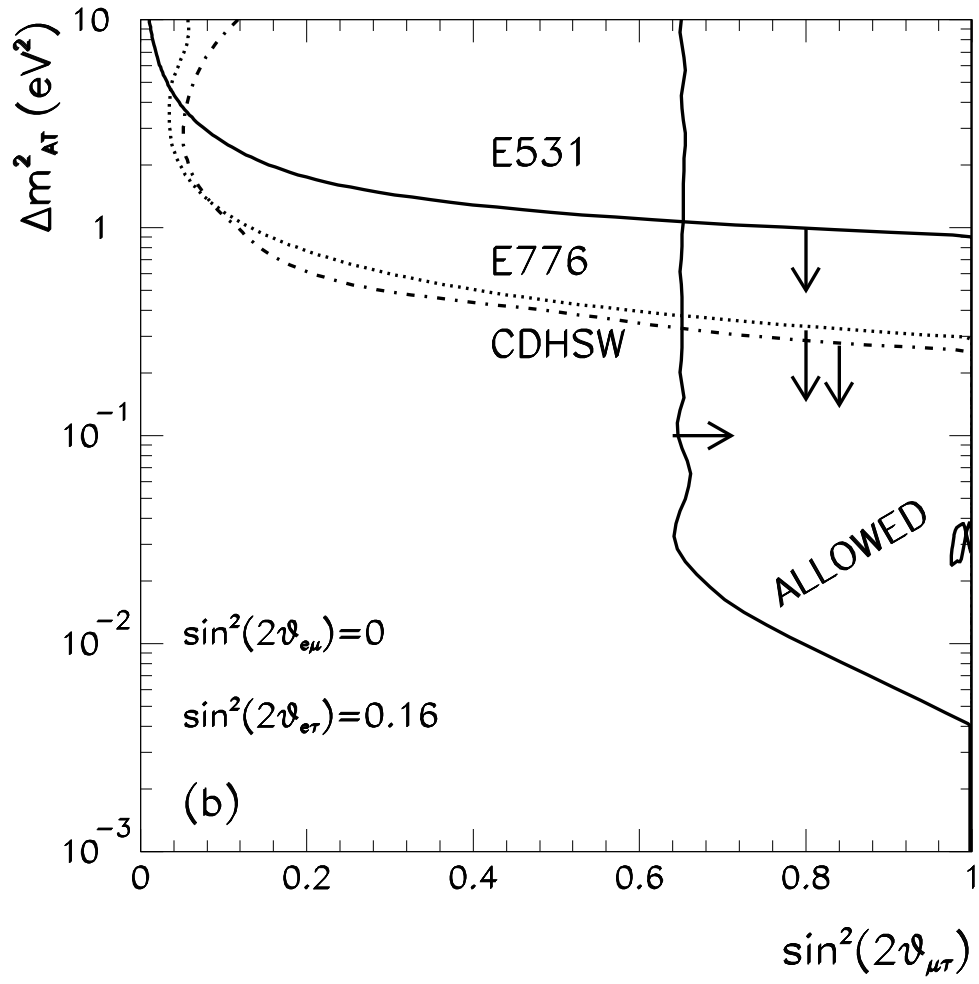


FIG. 2. (a) The 2σ allowed regions in the Δm^2_{AT} , $\sin^2(2\theta_{\mu\tau})$ plane for the atmospheric neutrino experiments for zero mixing $e\tau$ and allowed values of mixing $e\mu$: Fréjus (solid line), Kamiokande sub-GeV events (dashed line), IMB (dotted line), and Kamiokande multi-GeV events (dot-dashed line). The arrows point towards the allowed regions for the different experiments. The thick solid line surrounds the 2σ allowed region for the combination of all experiments.

(b). Allowed region from the atmospheric neutrino deficit analysis together with the relevant constraints from the laboratory experiments for zero mixing $e\tau$ and allowed values of mixing $e\mu$.





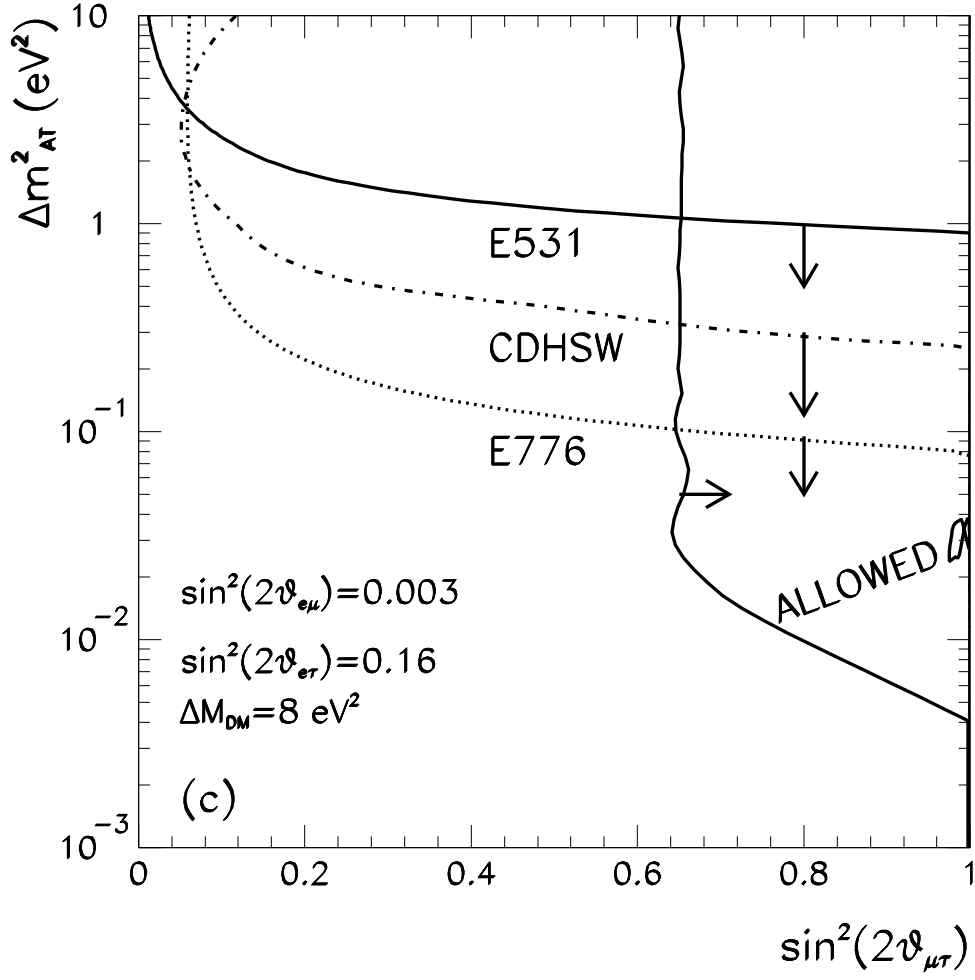


FIG. 3. (a) Same as Fig. 2.a for maximum allowed mixing $e\tau$ and allowed values of the mixing $e\mu$.
 (b) Same as Fig. 2.b for maximum allowed mixing $e\tau$ and allowed values of the mixing $e\mu$.
 (c). Same as (b) but for maximum allowed mixing $e\mu$ and corresponding allowed value for ΔM_{DM}^2 from the E776 experiment data.

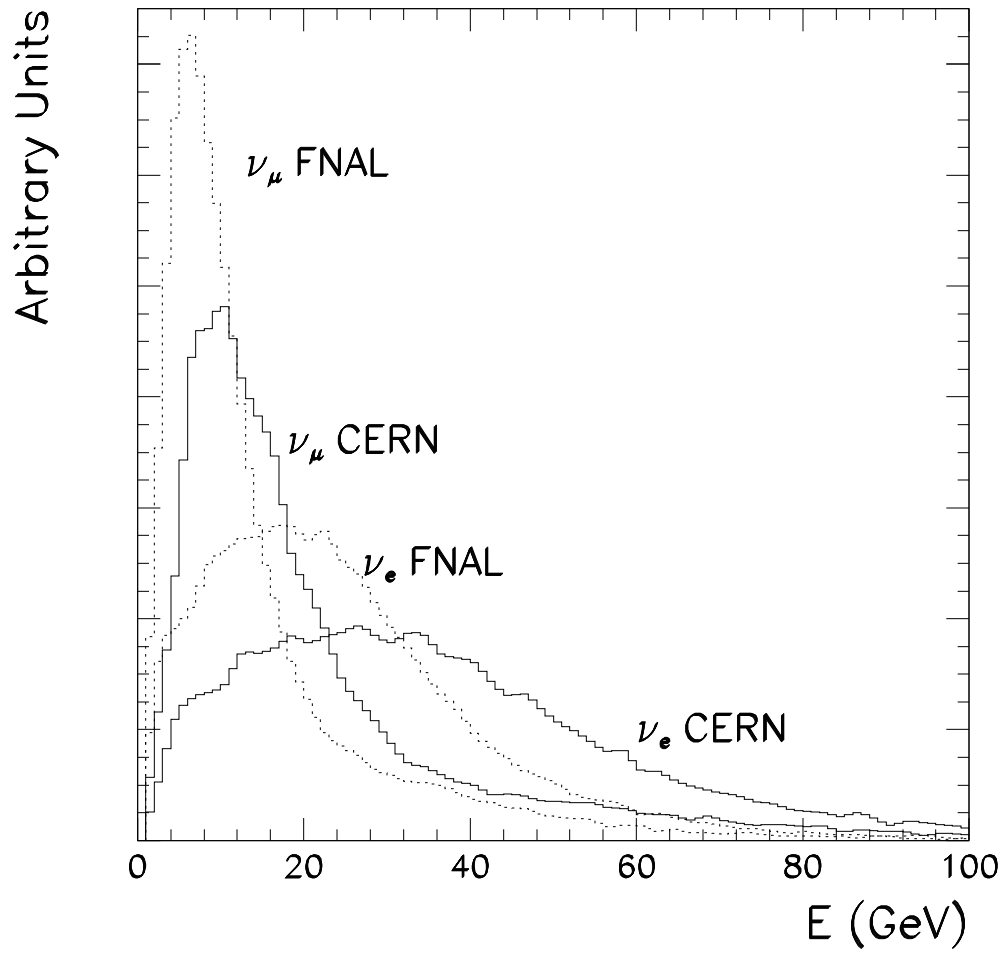


FIG. 4. ν_e and ν_μ spectra for the CERN beam (solid lines) and the Fermilab beam (dashed lines) as labeled.

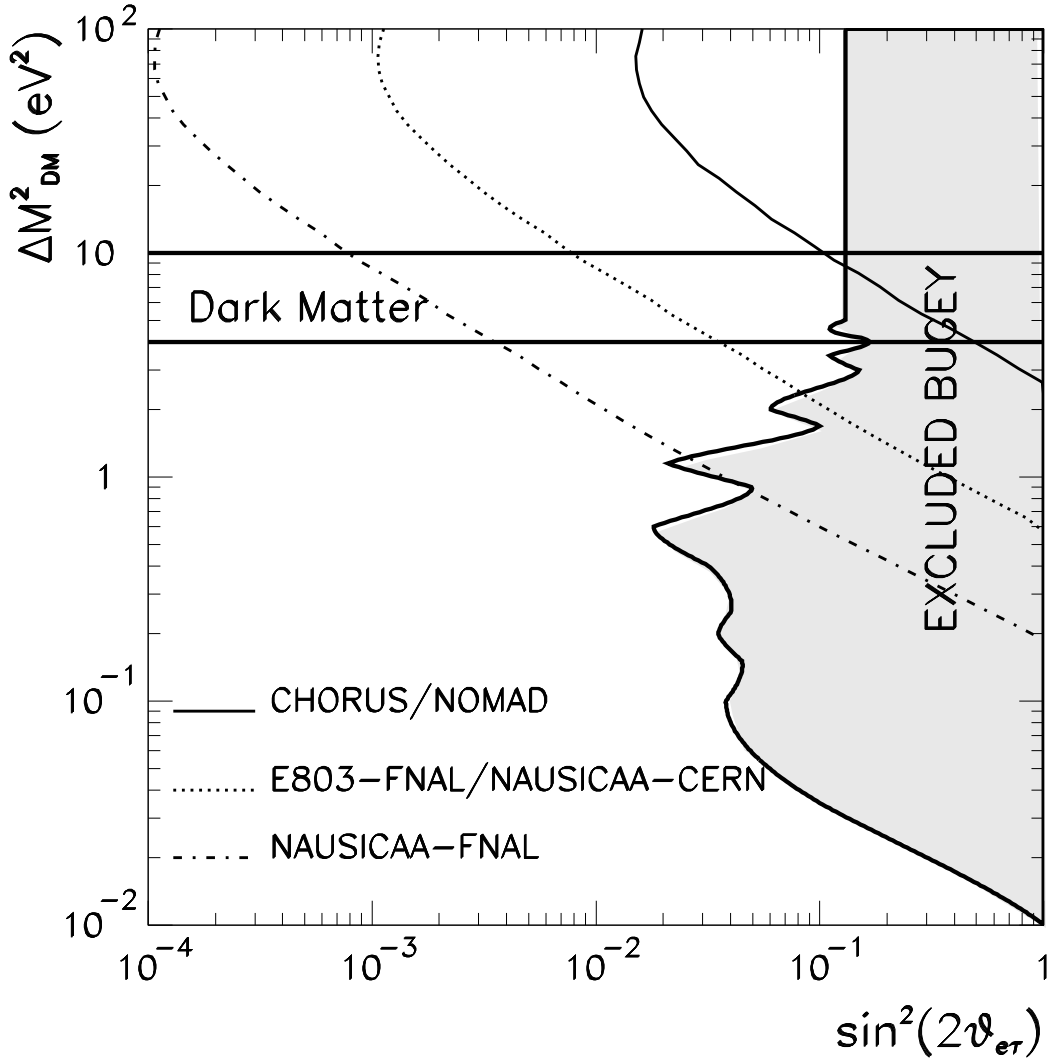


FIG. 5. Accessible regions (90% CL) for the $\nu_e \rightarrow \nu_\tau$ oscillation in the $(\Delta M_{DM}^2, \sin^2(2\theta_{e\tau}))$ plane for the CHORUS/NOMAD experiments (fine solid line) and Fermilab experiment E803/the improved CERN experiment (dotted line). The dot-dashed line delimits the region accessible to NAUSICAA at Fermilab. Also shown in the figure are the region at present excluded by the Bugey data (shaded area) and the favoured range on ΔM_{DM}^2 from dark matter considerations (solid horizontal lines).

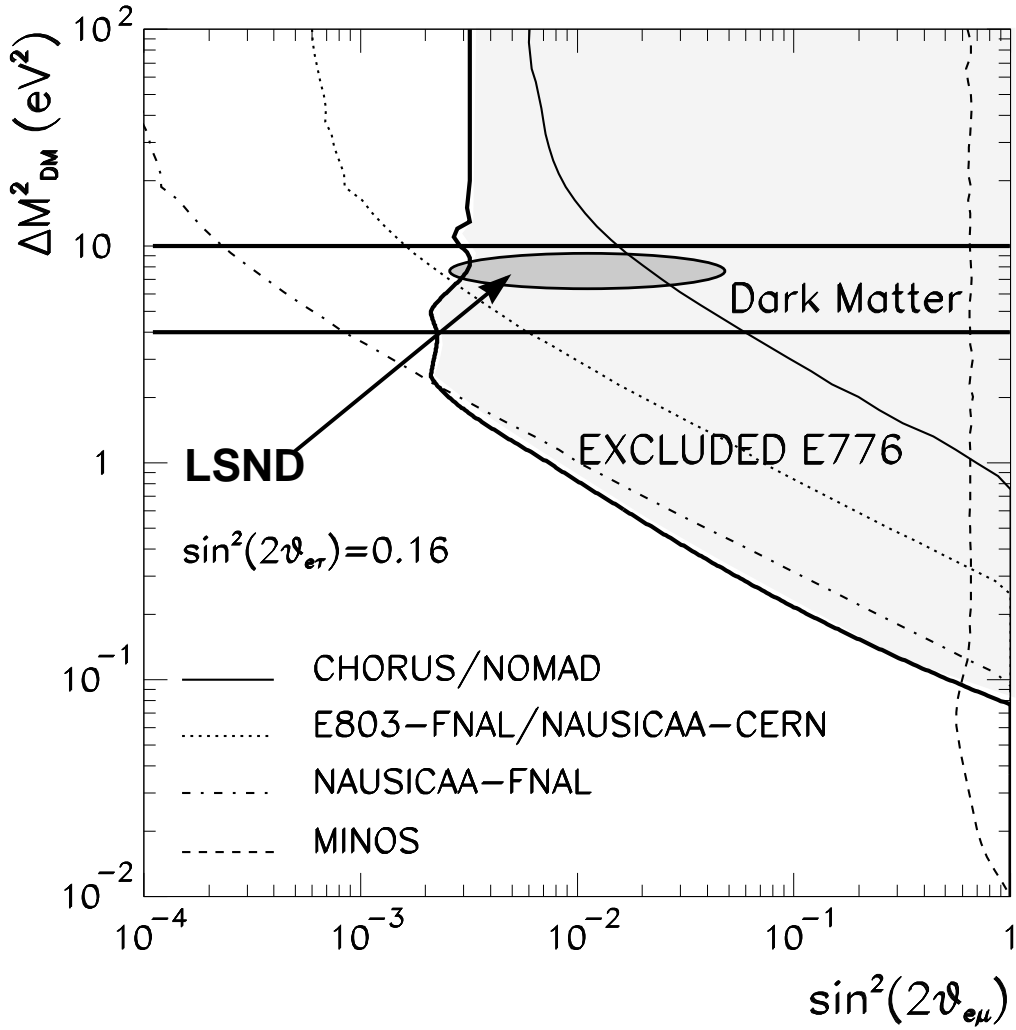
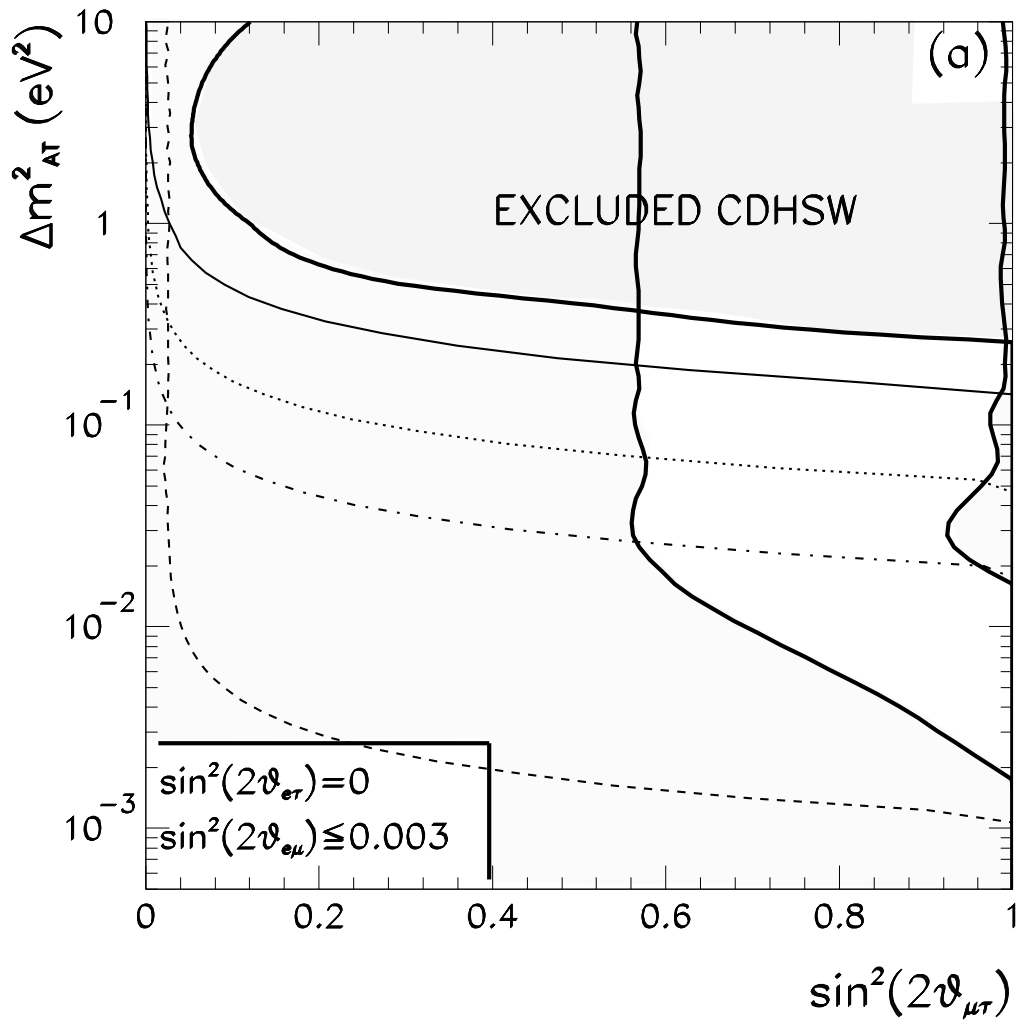


FIG. 6. Accessible regions (90% CL) for the $\nu_\mu \rightarrow \nu_\tau$ oscillation in the $(\Delta M_{DM}^2, \sin^2(2\theta_{e\mu}))$ plane for an optimum value of the mixing $e\tau$. The fine solid line corresponds to the CHORUS/NOMAD experiments and the dotted line corresponds to the Fermilab experiment E803 and to the improved CERN experiment. The dot-dashed line corresponds to NAUSICAA at Fermilab and the dashed line corresponds to MINOS. Also shown in the figure are the regions at present excluded by E776 data (shaded area) and the favoured range on ΔM_{DM}^2 from dark matter considerations (solid horizontal lines). For comparison also the LSND data are shown.



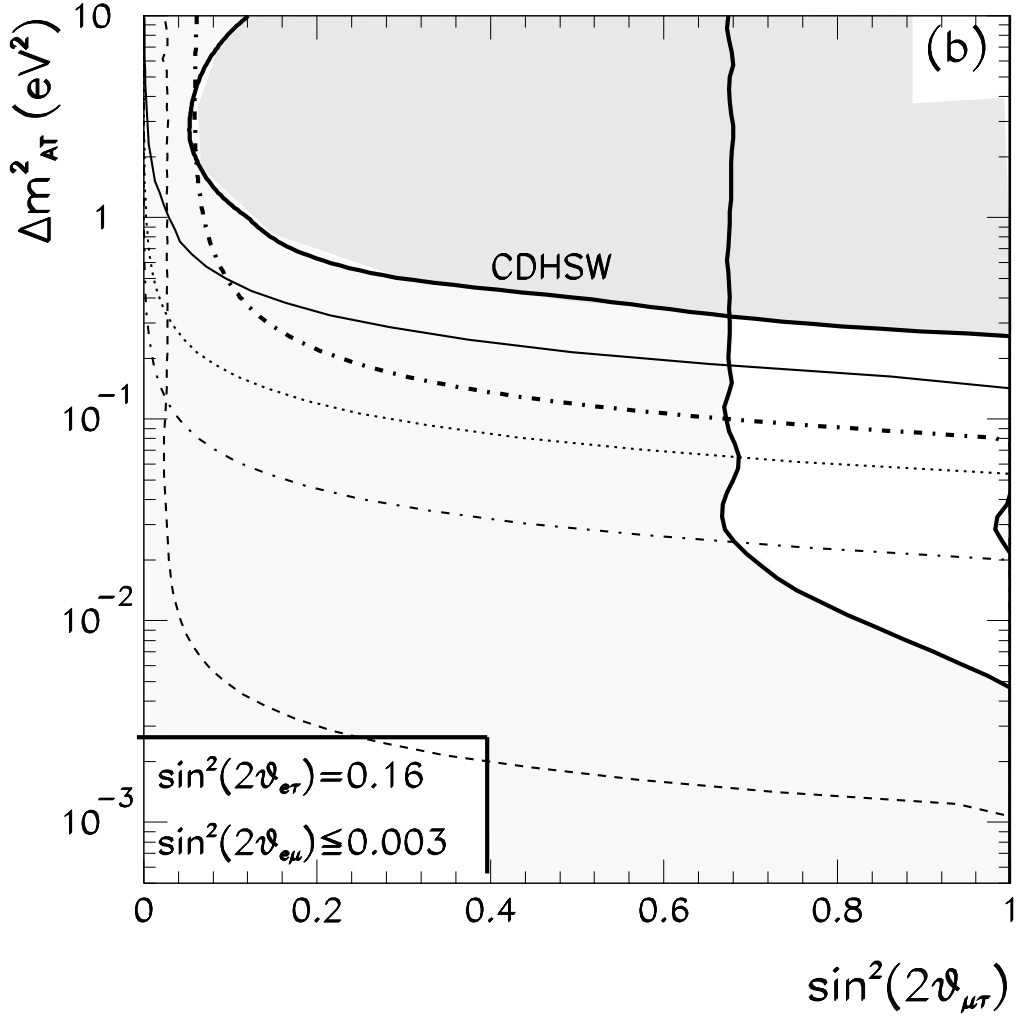


FIG. 7. (a) Accessible regions (90% CL) for the $\nu_\mu \rightarrow \nu_\tau$ oscillation in the $(\Delta m_{AT}^2, \sin^2(2\theta_{\mu\tau}))$ plane for zero value of the mixing $e\tau$. The fine solid line corresponds to the CHORUS/NOMAD experiments and the dotted line corresponds to the Fermilab experiment E803 and to the improved CERN experiment. The dot-dashed line corresponds to NAUSICAA at Fermilab and the dashed line to MINOS. Also shown in the figure are the regions at present excluded by CDHSW data (dark shaded area) and the atmospheric neutrino analysis (light shaded area).

(b) Same as (a) for maximum mixing $e\tau$. Also shown in the figure are the region at present excluded by CDHSW data (dark shaded area) and the atmospheric neutrino analysis (light shaded area). These are the only constraints for zero or values of the $e\mu$ mixing $\sin^2(2\theta_{e\mu}) \ll 0.003$. For maximum value $\sin^2(2\theta_{e\mu}) \simeq 0.003$ the E776 limit (thick dot-dashed line) is relevant.